Front. Electr. Electron. Eng. China 2008, 3(1): 55–60
DOI 10.1007/s11460-008-0002-x

RESEARCH ARTICLE

Junyuan LI, Hongjun CHEN, Shengfeng LI, Xiaohua ZHANG

Localization technique research of a pipeline robot based on the magnetic-dipole model

Abstract The magnetic field distribution of an emission antenna is studied in this paper. When the slenderness ratio of the emission antenna is high, the emission antenna can be simplified as a magnetic dipole for practical application. The numerical results of the magnetic dipole magnetic field show that the magnetic magnitude distribution has a hump-shape, whose direction is perpendicular with the antenna axis direction. A localization method based on the hump-shape signal detection is presented. The experimental result shows that the precision can reach a value of ± 5 cm. The method can be used to localize a pipeline robot working in a metal pipe.

Keywords low frequency electromagnetic wave, magnetic dipole, localization, pipeline robot

1 Introduction

Along with the development of pipeline transportation, the requirement of pipeline inspection becomes much higher especially for inner pipeline destructive inspection and pipeline clearance. Because a pipeline has the particularities of obstruction, anoxic condition and narrow space, it is difficult to conduct pipeline inspection using manual methods given such poor conditions. Thus, the technology of using pipeline robots has been widely adopted in the fields such as metal pipeline welding line inspection, urban water pipeline inspection and oil transportation pipeline inspection [1–4].

Oil from the seabed has to be transported in a pipeline buried underneath. Therefore, the inspection and on-line maintenance of seabed oil transporting pipeline are significant for the exploration of sea oil. A seabed pipeline robot moves in the pipeline and inspects the pipeline with sensors using inner source mode. Manual disposal and succor is in demand when there are deficiencies in the pipeline or when there is a malfunction in the robot. Thus, handlers outside the pipeline should know the precise location of the robot and then take corresponding measures. Therefore, outer localization of the inner moving robot has become one of the most important technologies in practical applications. Moreover, it is one of the most important issues in the industrialization of pipeline robots.

The traditional localization method is to use γ ray which has a good performance of penetration. Because γ ray is radioactive, it can not only destroy the sea environment, but also do serious harm to the health of the handlers. Because ultra-low-frequency electromagnetic wave provides good penetration in the steel pipeline, mud, and water, it has been widely used in the fields of pipeline engineering, mine communication, object localization, and measurement [5–10]. This paper analyzes the magnetic field distribution of an ultra-low-frequency (ULF) electromagnetic wave and magnetic dipole model. That is, when the distance between the field point and the axis of emission coil stays invariable, the amplitude of the magnetic field intensity that is vertical to the emission antenna direction has a hump-shape with the changed horizontal distance. Based on the rule of hump-shape, a method for the location of the inner mobile robot from outside the pipeline is proposed.

2 The magnetic field of emission antenna

Because the frequency of ultra-low-frequency electromagnetic wave is much lower, the radiant process of the

Translated from *Chinese Journal of Radio Science*, 2006, 21(4): 553–557 [译自: 电波科学学报]

Junyuan LI (✉)
Department of Electrical Engineer, Harbin Institute of Technology, Weihai 264209, China
E-mail: lijunyuan@hit.edu.cn

Hongjun CHEN, Xiaohua ZHANG
Department of Electrical Engineer, Harbin Institute of Technology, Harbin 150001, China

Shengfeng LI
Department of Physics, Harbin Institute of Technology, Weihai 264209, China

electromagnetic wave is fulfilled via the changing magnetic field of an emission coil. Therefore, analyzing the magnetic field of an emission coil is one of the theoretical principles of studying the signal magnitude of a receiving antenna along with the changing of the antenna location. Moreover, it is the theoretical argument for inspecting the location of the inner mobile robot outside the pipeline with ultra-low-frequency electromagnetic wave.

An ultra-low-frequency electromagnetic wave emission antenna can be regarded as a compact solenoid of a finite length. Traditional teaching materials [11] and a good number of literature only present the magnetic field distribution of the axis direction of a solenoid of infinite length or finite length. However, in practical application, the length of the solenoid is finite, therefore we should analyze the magnetic field distribution of a solenoid with finite length.

Taking the center of the solenoid as the origin of the coordinates and the axis direction of the solenoid as z axis, we can set up an $Oxyz$ Cartesian coordinate system, as shown in Fig. 1. The length of the solenoid is $2l$, the radius is r, current is I, and the number of the circular loop wire is n.

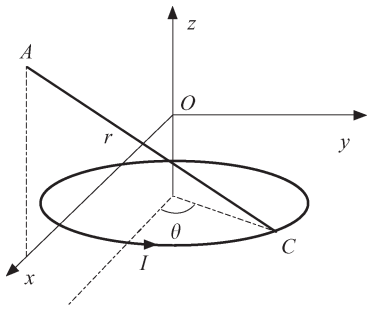

Fig. 1 Magnetic field of solenoid

The magnetic field distribution of the solenoid is reflection-symmetric, so the magnetic field distributions of the field points, which are vertical to the axis plane and with equal distances to axis, have the same amplitude and symmetrical directions. For convenient analysis without losing generality, discussing magnetic field distribution of field points in Oxz plane can directly set up the integrated magnetic field distribution of the solenoid.

According to the Biot-Savart law [11], the magnetic field intensity $\mathrm{d}\boldsymbol{B}$ at field point $A(x_0, 0, z_0)$, which is generated from the unit current line $I\mathrm{d}L$ at point C ($R\cos\theta$, $R\sin\theta$, z), can be expressed in Eq. (1):

$$\mathrm{d}\boldsymbol{B}=\frac{\mu_0}{4\pi}\frac{In\mathrm{d}z\mathrm{d}\boldsymbol{L}\times\boldsymbol{r}}{r^3}. \tag{1}$$

Here, I is the current of the circular line, n is the number of the circular loop wire, r is the radius of the circular line, and μ_0 is the magnetic conductive rate in free space.

By using vector calculation and Eq. (1), the magnetic filed $\mathrm{d}\boldsymbol{B}$ can be written as Eq. (2):

$$\begin{aligned}\mathrm{d}\boldsymbol{B}&=\frac{\mu_0}{4\pi}\frac{In\mathrm{d}z\mathrm{d}\boldsymbol{L}\times\boldsymbol{r}}{r^3}\\&=\frac{\mu_0}{4\pi}\frac{In\mathrm{d}z(-R\sin\theta d\theta\boldsymbol{i}+R\cos\theta d\theta\boldsymbol{j})}{\left((x_0-R\cos\theta)^2+(-R\sin\theta)^2+(z_0-z)^2\right)^{3/2}}\\&\quad\times[(x_0-R\cos\theta)\boldsymbol{i}+(-R\sin\theta\boldsymbol{j})+(z_0-z)\boldsymbol{k}].\end{aligned} \tag{2}$$

Here, θ is the angle between the x axis and radius at point C.

Then, according to Eq. (2), the components $\mathrm{d}B_x$ and $\mathrm{d}B_z$ along x and z axis of $\mathrm{d}\boldsymbol{B}$ can be written as:

$$\mathrm{d}B_x=\frac{\mu_0 In\mathrm{d}z}{4\pi}\frac{(z_0-z)R\cos\theta}{\left(R^2-2R\cos\theta x_0+x_0^2+(z_0-z)^2\right)^{3/2}}\mathrm{d}\theta, \tag{3}$$

$$\mathrm{d}B_z=\frac{\mu_0 In\mathrm{d}z}{4\pi}\frac{R(R-x_0\cos\theta)}{\left(R^2+x_0^2-2R\cos\theta x_0+(z_0-z)^2\right)^{3/2}}\mathrm{d}\theta. \tag{4}$$

Carrying out the integral on Eq. (3), then the component B_x along the x axis of $\boldsymbol{B}$ can be written as follows:

$$\begin{aligned}B_x&=\frac{\mu_0 In}{4\pi}\int_{-l}^{l}\mathrm{d}z\int_{-\pi}^{\pi}\frac{R(z_0-z)\cos\theta\mathrm{d}\theta}{\left(R^2-2R\cos\theta x_0+x_0^2+(z_0-z)^2\right)^{3/2}}\\&=\frac{\mu_0 InR}{4\pi}\int_{-\pi}^{\pi}f(\theta)\mathrm{d}\theta,\end{aligned} \tag{5}$$

where

$$\begin{aligned}f(\theta)&=\frac{\cos\theta}{\left(R^2-2R\cos\theta x_0+x_0^2\right)^{1/2}}\\&\quad\times\left(\frac{1}{\left(R^2-2R\cos\theta x_0+x_0^2+(z_0+l)^2\right)^{1/2}}\right.\\&\quad\left.-\frac{1}{\left(R^2-2R\cos\theta x_0+x_0^2+(z_0-l)^2\right)^{1/2}}\right).\end{aligned}$$

In the same way, the component B_z along the z axis of $\boldsymbol{B}$ can be expressed as Eq. (6):

$$\begin{aligned}B_z&=\frac{\mu_0 In}{4\pi}\int_{-l}^{l}\mathrm{d}z\int_{-\pi}^{\pi}\frac{R(R-x_0\cos\theta)\mathrm{d}\theta}{\left(R^2+x_0^2-2R\cos\theta x_0+(z_0-z)^2\right)^{3/2}}\\&=\frac{\mu_0 InR}{4\pi}\int_{-\pi}^{\pi}g(\theta)\mathrm{d}\theta,\end{aligned} \tag{6}$$

where

$$g(\theta)=\frac{-(R-x_0\cos\theta)}{\left(R^2-2R\cos\theta x_0+x_0^2\right)}\times\left(\frac{z_0-l}{\left(R^2-2R\cos\theta x_0+x_0^2+(z_0-l)^2\right)^{1/2}}-\frac{z_0+l}{\left(R^2-2R\cos\theta x_0+x_0^2+(z_0+l)^2\right)^{1/2}}\right).$$

In engineering implementation, Eqs. (5) and (6) should be simplified, which can not only maintain the distribution rule of the magnetic field, but also make computation simpler. Consider the case $2l \gg R$, a solenoid can be referred to as a magnetic dipole [12]. The dipole is composed of a couple of magnetic charges $\pm qm$ which have different signs under equal quantity. The magnetic field of this dipole is shown in Fig. 2.

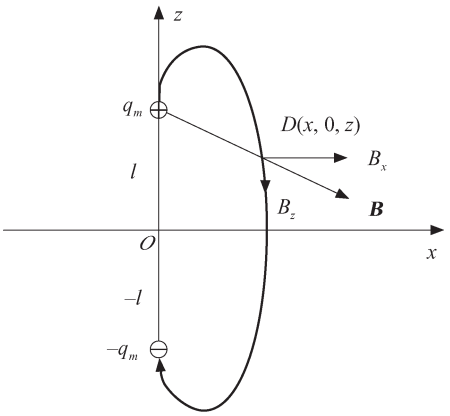

Fig. 2 Magnetic field of a magnetic dipole

If the length of the circular loop is $2l$, then the moment of the magnetic dipole is expressed as Eq. (7) and the capacity of the magnetic charge is expressed as Eq. (8):

$$m=2nlIS, \tag{7}$$

$$q_m=\frac{m}{2l}=nI\pi R^2. \tag{8}$$

The components along the x axis and z axis of magnetic field $\boldsymbol{B}$ at point $D(x, 0, z)$ generated by positive magnetic charge $+q_m$ can be expressed as Eqs. (9) and (10):

$$B_{x(+q)}=\frac{\mu_0}{4\pi}\frac{q_m x}{\left(x^2+(l-z)^2\right)^{3/2}}, \tag{9}$$

$$B_{z(+q)}=\frac{\mu_0}{4\pi}\frac{q_m(z-l)}{\left(x^2+(z-l)^2\right)^{3/2}}. \tag{10}$$

The components along the x axis and z axis of magnetic field $\boldsymbol{B}$ at point D generated by negative magnetic charge $-q_m$ can be expressed as Eqs. (11) and (12):

$$B_{x(-q)}=\frac{\mu_0}{4\pi}\frac{-q_m x}{\left(x^2+(l+z)^2\right)^{3/2}}, \tag{11}$$

$$B_{z(-q)}=\frac{\mu_0}{4\pi}\frac{-q_m(z+l)}{\left(x^2+(z+l)^2\right)^{3/2}}. \tag{12}$$

The magnetic field at point D is generated by magnetic charge q_m and $-q_m$ following parallelogram law. According to Eqs. (9) and (11), the component along the x axis of $\boldsymbol{B}$ at point D generated by the dipole can be expressed as Eq. (13):

$$B_x=\frac{nIR^2\mu_0 x}{4}\left(\frac{1}{\left(x^2+(l-z)^2\right)^{3/2}}-\frac{1}{\left(x^2+(l+z)^2\right)^{3/2}}\right). \tag{13}$$

In the same way, according to Eqs. (10) and (12), the component along the z axis of $\boldsymbol{B}$ at point D generated by the dipole can be expressed as Eq. (14):

$$B_z=\frac{nIR^2\mu_0}{4}\left(\frac{z-l}{\left(x^2+(z-l)^2\right)^{3/2}}-\frac{z+l}{\left(x^2+(z+l)^2\right)^{3/2}}\right). \tag{14}$$

Equations (13) and (14) characterize the magnetic field at point D generated by the dipole. According to Eqs. (13) and (14), we can analyze the magnetic field distribution of a field point along the x axis and z axis. The basic parameters of the solenoid are listed in Table 1.

Table 1 Basic parameters of solenoid

length $2l$/mm	radius R/mm	current I/A	number n/mm
200	20	0.1	500

Denoting $x = 1$ m, the component B_x along the x axis of the magnetic field changes with alterations of z axis, and the corresponding curve is illustrated in Fig. 3.

It is shown in Fig. 3 that when z is near the origin, the component B_x along the x axis increases when z increases, and the sign is the same as z. This

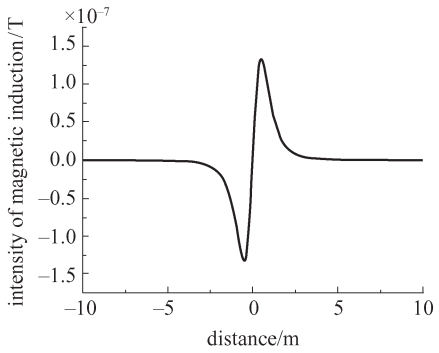

Fig. 3 Relationship between B_x and z

relationship is the basic principle for the pipeline robot localization.

3 Localization with ULF electromagnetic wave

Seabed oil transportation pipeline inspection robot moves in the pipeline according to a predetermined order, inspecting the condition of the pipeline. The succor equipment on the sea moves along the pipelines under the help of pipeline tracking devices, and tracks the location of the pipeline robot with the help of localization devices, as shown in Fig. 4.

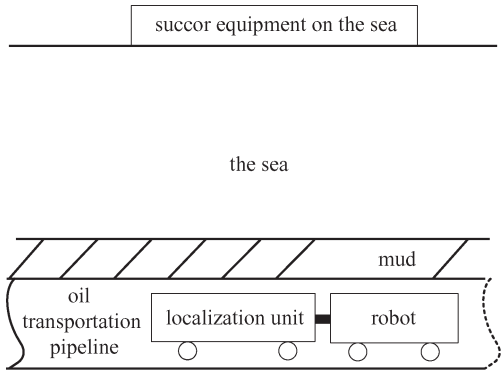

Fig. 4 Sketch map of localization of pipeline robot

When a pipeline fault, power interruption, or other abnormal cases occur, the robot will remain in the inspected pipeline, and await disposal from a succor equipment on the sea. Meanwhile, the ultra-low-frequency (ULF) electromagnetic wave is needed to locate the pipeline robot accurately, while the equipment on the sea takes care of the malfunction and ensures unhindered inspection of the pipeline.

The ULF electromagnetic wave emission antenna is installed on the pipeline robot parallel to the axis direction of the pipeline. The ULF electromagnetic wave receiving antenna is installed on the succor equipment on the sea vertical to the emission antenna.

Because the radius of the solenoid ($r = 20$ mm) is much shorter than its length ($2l = 200$ mm), the magnetic field of the solenoid can be regarded as that of a dipole. According to Eq. (13), the relationship between $|B_x|$ and z axis is shown in Fig. 5.

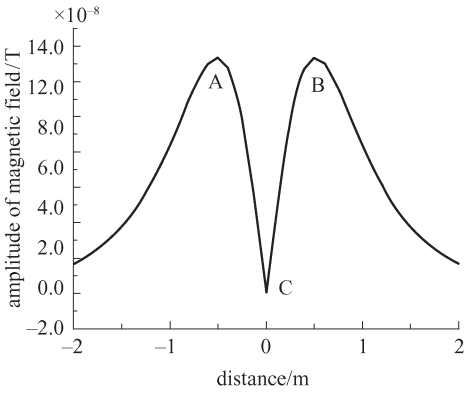

Fig. 5 Relationship between $|B_x|$ and z

According to Fig. 5, $|B_x|$ is a hump-shape as z changes. The location of the minimum value point C of the hump signal corresponds with that of the electromagnetic wave emitter.

During the process of locating, the receiving antenna receives amplitude signals vertical to the direction of the magnetic field changing of the emission antenna through the LC resonant circuit, which is shown in Fig. 6.

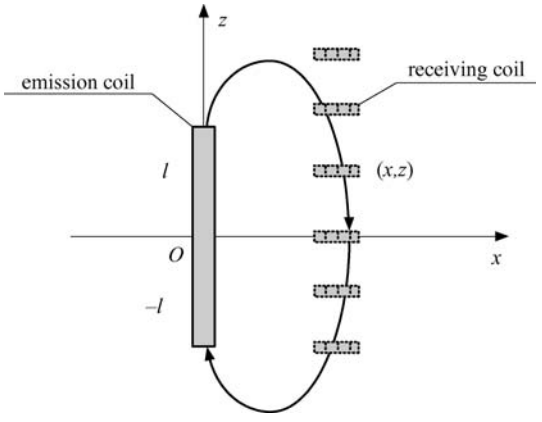

Fig. 6 Magnetic field when locating

With the relative location changing between the receiving and emission antennas, the magnitude of the signal on the receiving antenna changes correspondingly. By inspecting the change of the magnitude of the signal and finding the location of the minimum point between the two humps (i.e., the location of the emitter), the

location of the robot inside the pipeline can be determined.

4 Experiment and analysis

According to the method of localization with the ULF electromagnetic wave, we designed a localization equipment. The basic parameters of the experiment condition are listed in Tables 1 and 2.

Table 2 Basic parameters of pipeline

length of pipeline/mm	diameter of pipeline/mm	thickness of pipeline/mm
4000	225	7.5

The current resolution of the emission coil is $I = 0.1\sin(1.4\pi t)\sin(46\pi t)$. Both terminals of the pipeline are sealed by using metal plugs. The vertical distance between the receiving and emission antennas is 1 m. Keeping the emission antenna static, the receiving antenna moves at 20 mm/s. Then, the output voltage signal of the receiving antenna is collected by an S7-300 PLC from SIEMENS. The experiment curve is shown in Fig. 7. The abscissa in the figure is the axis distance between the receiving and emission antennas.

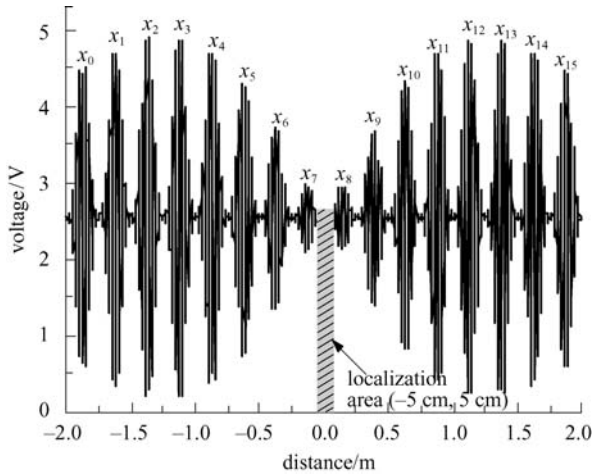

Fig. 7 Localization experiment with ULF electromagnetic wave

16 local maximum value points $x_0 - x_{15}$ of $\sin(1.4\pi t)$ envelope are chosen, which are shown in Fig. 7 and Table 3.

The distribution trend of the points on the envelope conforms to the trend of the double humps signal of Fig. 5 within the area (−2 m, 2 m). The voltages at points x_7 and x_8 are the minimum, and the corresponding area between x_7 and x_8 is the localization area.

Table 3 Envelope points value

envelope points	x_0	x_1	x_2	x_3	x_4	x_5	x_6	x_7
distance/m	1.86	1.63	1.36	1.13	0.86	0.63	0.39	0.14
voltage/V	4.51	4.70	4.88	4.85	4.70	4.28	3.74	2.98
envelope points	x_8	x_9	x_{10}	x_{11}	x_{12}	x_{13}	x_{14}	x_{15}
distance/m	0.13	0.38	0.63	0.86	1.10	1.38	1.60	1.86
voltage/V	2.95	3.70	4.34	4.70	4.87	4.78	4.67	4.47

Because noise is contained in the signal, the computed result of the minimum value points between the double humps is an area around the minimum value. The gray area in Fig. 7 is the localization area, i.e., the location corresponding to this area is the location of the ULF electromagnetic wave emission antenna. The result of the experiment shows that the location span of this area is (−5 cm, 5 cm), so the experiment precision of localization can achieve ±5 cm.

5 Conclusions

This paper analyzes the magnetic field distribution of a ULF electromagnetic wave emission antenna based on electromagnetism. Furthermore, the emission antenna is regarded as a magnetic dipole so as to be implemented in engineering, and the resolution becomes simple and practical.

Based on the resolution of the magnetic field distribution of the dipole, the magnetic field distribution vertical to the direction of the dipole can be computed. Also, the numerical calculated results show that the magnetic magnitude of the vertical direction has a hump-shape with the change of distance between the field point and the axis of the dipole. According to the actual utilization and characteristics of the magnetic field distribution, this paper proposes a localization method based on the ULF magnetic wave with hump-shape.

Experiment results show that the ULF magnetic wave localization based on the dipole model has high precision (being able to achieve ±5 cm). It can satisfy the demand of localization of the pipeline robot outside the pipeline in pipeline engineering.

Acknowledgements This work was supported by the Hi-Tech Research and Development Program of China (Grant No. 2001AA602021).

References

1. Moraleda J, Ollero A, Orte M. A robotic system for internal inspection of water pipelines. IEEE Robotics & Automation Magazine, 1999, 6(3): 30–41
2. Vradis G, Schempf H. Robotic system inspects live gas mains. Gas Industries, 2004, 48(8): 16–18
3. Anon. Measuring bending stress in buried metal gas pipes. Journal of Failure Analysis and Prevention, 2004, 4(4): 6–7

4. Roh Se-Gon, Choi H R. Differential-drive in-pipe robot for moving inside urban gas pipelines. IEEE Transactions on Robotics, 2005, 21(1): 1–17
5. Tang J F, Gong S G, Wang J G. Two new magnetic localization and parameter estimation methods under the dipole model. ACTA Electronica Sinica, 2003, 31(1): 154–157 (in Chinese)
6. Xu J R, Xue L. LS algorithm used in DF and location. Chinese Journal of Radio Science, 2001, 16(2): 227–230 (in Chinese)
7. Ren Z L, Huang Y Y, Chen Z M. Passive ranging and tracking method for magnetic dipole source. Journal of Data Acquisition & Processing, 2001, 16(3): 380–383 (in Chinese)
8. Deng P, Li L, Fan P Z. A hybrid TDOA/AOA location algorithm and its performance analysis. Chinese Journal of Radio Science, 2002, 17(6): 633–636 (in Chinese)
9. Sun Y C, Zheng H, Cui Y H. The multilayer case-pipes electromagnetic defect detection logging. Well Logging Technology, 2003, 27(3): 246–264 (in Chinese)
10. Liu Q B, Liu J X. Station location based on radio direction-finding. Chinese Journal of Radio Science, 2003, 18(2): 211–215 (in Chinese)
11. Zhao K H, Chen X M. Electromagnetism. Beijing: Higher Education Press, 1990 (in Chinese)
12. Guo S H. Electromotive Power. Beijing: Higher Education Press, 1997 (in Chinese)